Astrophysical reaction rates with realistic nuclear level densities

Sangeeta¹, T. Ghosh^{2,3}, B. Maheshwari^{4,5}, G. Saxena^{6,*}, B. K. Agrawal^{2,3}

¹Department of Applied Sciences, Chandigarh Engineering College, Landran-140307, India

²Saha Institute of Nuclear Physics, Kolkata-700064, India

³Homi Bhabha National Institute, Anushakti Nagar, Mumbai-400094, India

⁴Department of Physics, Faculty of Science, University of Zagreb, HR-10000 Zagreb, Croatia

⁵Department of Physics, Indian Institute of Technology Ropar, Rupnagar-140001, India and

⁶Department of Physics (H & S), Govt. Women Engineering College, Ajmer-305002, India*

(Dated: March 30, 2022)

Realistic nuclear level densities (NLDs) obtained within the spectral distribution method (SDM) are employed to study nuclear processes of astrophysical interest. The merit of SDM lies in the fact that the NLDs corresponding to many body shell model Hamiltonian consisting of residual interaction can be obtained for the full configurational space without recourse to the exact diagnolization of huge matrices. We calculate NLDs and s-wave neutron resonance spacings which agree reasonably well with the available experimental data. By employing these NLDs, we compute reaction cross-sections and astrophysical reaction rates for radiative neutron capture in few Fe-group nuclei, and compare them with experimental data as well as with those obtained with NLDs from phenomenological and microscopic mean-field models. The results obtained for the NLDs from SDM are able to explain the experimental data quite well. These results are of particular importance since the configuration mixing through the residual interaction naturally accounts for the collective excitations. In the mean-field models, the collective effects are included through the vibrational and rotational enhancement factors and their NLDs are further normalized at low energies with neutron resonance data.

I. INTRODUCTION

Neutron capture reactions are critical for a wide variety of applications ranging from medicine [1], energy generation [2] to nucleosynthesis [3]. Such reactions are fundamentally important by which nearly all of the elements heavier than iron are synthesized through astrophysical s-process or r-process. The astrophysical site where the rprocess occurs has been one of the major open questions for last several decades. Supernovae and neutron star mergers are the most favored astrophysical sites for the r-process. Only recently, observations connected to the neutron star merger event GW170817 [4] have confirmed the emission of a kilonova afterglow which is powered by the radioactive decay of heavy nuclides produced in the r-process [5, 6]. Efforts are also being made to simulate the neutron capture nucleosynthesis in the laboratory [7]. This led to a rapid increase in attention on various processes contributing to nuclear reaction network.

The extensive radiative neutron capture cross-section data are crucial for complete understanding of r-process nuclear astrophysical network calculations. All such data are not accessible in the accelerator-based experiments and one needs to rely on theoretical estimates. The reaction cross-sections and relevant reaction rates are calculated within a statistical framework [8] which primarily requires (i) neutron-nucleus optical model potential (OMP), (ii) γ -ray strength function (γ SF), and (iii) nuclear level density (NLD). The uncertainties of γ SF and NLD have significant impact on calculated neutron cap

ture rates while the uncertainties due to OMP are relatively smaller [9, 10]. The NLD describes the total number of states accessible in a given nucleus at a specific excitation energy. Various methods have been employed to calculate the NLDs which range from simple phenomenological models based on non-interacting degenerate Fermi gas [11, 12] to more complex mean-field descriptions [13]. In the mean-field approaches, all the collective effects are incorporated in NLDs through the rotational and vibrational enhancement factors. These NLDs are further normalized with the experimental data at the neutron resonances [13]. In the shell model, the configuration mixing through the residual interaction naturally accounts for the collective excitations.

There are a few approaches to calculate the NLDs within the framework of shell model. One of them is the shell model Monte Carlo (SMMC) [14–19], which utilizes auxiliary fields to compute the thermal trace for the energy and then NLDs are obtained using inverse Laplace transform. Another approach to calculate the spin and parity dependent shell model level densities is developed using the spectral distribution method (SDM) [20–25]. This method allows one to incorporate the many-body effects on the wave functions appropriately and is a basis for the applications of statistical spectroscopy generated by many-body chaos, as modeled by embedded random matrix ensembles, along with the studies on beta decay rates for stellar evolution and supernovae [26–29]. Recently, the SDM has been extended for the exact calculation of the first and second Hamiltonian moments for different configurations at fixed spin and parity [30–33]. This is a practical tool to construct the NLDs for many body shell model Hamiltonian using full configurational space since it avoids the diagonalization of Hamiltonian

 $[*]Electronic \ address: \ gauravphy@gmail.com\\$

matrices of huge dimensions. This method, however, requires an accurate estimation of the shell model ground state energy, which is generally as time consuming as the full shell model calculation. The difficulty has been overcome by using the exponential convergence method [34] or the recently developed projected configuration interaction method [35, 36]. The NLDs obtained from SDM also agree reasonably with the full shell model calculations [32]. Recently, extrapolated Lanczos method [37] has also been developed for an accurate computation of the level densities described within the configuration space.

In the present work, we use realistic NLDs obtained from spectral distribution method followed by an appropriate parity equilibration scheme for pf-model space to calculate the neutron capture reaction cross-sections and astrophysical reaction rates. We consider some of the (n,γ) processes consisting a few seed nuclei for the nucleosynthesis in and around the Fe-group for which experimental data are available. We compare our results with those obtained with NLDs from other phenomenological and microscopic models as commonly employed.

II. NUCLEAR LEVEL DENSITIES

The NLDs are obtained using spectral distribution method [32] applied to shell model Hamiltonian with a realistic residual interaction. Within the spectral distribution method, one calculates first and second moments of Hamiltonian for the full configurational space. These moments are then used to construct the Gaussian distribution of the levels which eventually give rise to the level density. For a given isotope (Z, N), the valence nucleons can be distributed in many ways over available orbitals. Each of these configurations is known as partition, p which contains $D_{\alpha p}$ many-body states with exact quantum numbers α . The states present in a given partition are distributed over some energy region as a result of interactions inside the partition. For each partition, the statistical average of an operator O over the states is defined through the corresponding trace,

$$\langle \hat{O} \rangle = \frac{1}{D_{\alpha p}} T r^{\alpha p} \hat{O} \tag{1}$$

In particular, the centroid energy of the partition is the first moment of the Hamiltonian,

$$E_{\alpha p} = \frac{1}{D_{\alpha p}} T r^{\alpha p} \hat{H} \tag{2}$$

This comes directly from the diagonal elements of the Hamiltonian matrix. The second moment of the Hamiltonian,

$$\sigma_{\alpha p}^2 = \langle H^2 \rangle_{\alpha p} - E_{\alpha p}^2 = \frac{1}{D_{\alpha p}} Tr^{\alpha p} H^2 - E_{\alpha p}^2$$
 (3)

is determined by the off-diagonal elements of the Hamiltonian matrix including the interaction between partitions. No matrix diagonalization is required as this quantity can be read directly from the Hamiltonian matrix.

The actual distributions are close to the Gaussians which is a manifestation of quantum complexity and chaotization [38–41]. Finally, the level density $\rho(E;\alpha)$ is found by summing the Gaussians weighted over their dimensions for all partitions at given energy E and with quantum numbers α ,

$$\rho(E;\alpha) = \sum_{p} D_{\alpha p} G_{\alpha p}(E) \tag{4}$$

The best results are obtained by using finite range or truncated Gaussians,

$$G_{\alpha p}(E) = G(E - E_{\alpha p} + E_{g.s.}; \sigma_{\alpha p})$$
 (5)

for each partition. Removing unphysical tails, the Gaus-

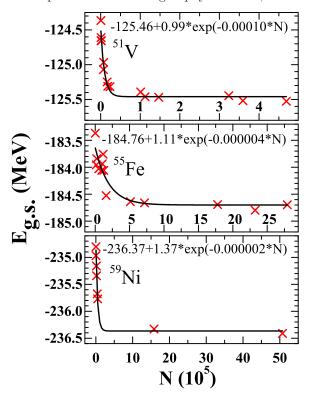


FIG. 1: Shell model ground state energies for 51 V, 55 Fe and 59 Ni corresponding to different truncations with dimensions N (red crosses). These energies are fitted to $a+be^{-cN}$ as indicated by solid line. The exponential converged ground state energies for full pf-model space are obtained using this fitted expression with $N=N_{full}$.

sians are cut off at a distance $\sim 2.6\sigma_{\alpha p}$ from the corresponding centroid and then re-normalized [32]. The ground state energies $E_{\rm g.s.}$ appearing in Eq. (5) must be calculated using full Hamiltonian matrix in order to be consistent with the first and second moments. Practically, it is convenient to calculate the invariant traces in the M-scheme. When $\rho(E;M)$ for a given parity is computed, the level density $\rho(E;J)$ for certain spin J is found as the difference of $\rho(M=J)$ and $\rho(M=J+1)$.

To illustrate, we have considered the reaction cross-sections for $^{50}{\rm V}(n,\gamma)^{51}{\rm V},~^{54}{\rm Fe}(n,\gamma)^{55}{\rm Fe},$ and

TABLE I: The ground state energies $E_{g.s.}$ (MeV) for different nuclei required to compute the cross-sections for the (n,γ) processes considered. The $E_{g.s.}$ are obtained using shell model Hamiltonian with GXPF1A residual interaction. The exponential convergence [34] is used for the cases where the full JT-space dimension (N_{full}) exceeds $\sim 5 \times 10^6$. The exponential converged value for 51 V is -125.46 MeV which is nearly equal to -125.54 MeV obtained for full model space calculation $(E_{g.s.}^{full})$.

	$^{50}\mathrm{V}(n,\gamma)^{51}\mathrm{V}$			$^{54}\mathrm{Fe}(n,\gamma)^{55}\mathrm{Fe}$			$^{58}\mathrm{Ni}(n,\gamma)^{59}\mathrm{Ni}$		
Channels	Nucleus	N_{full}	$E_{g.s.}$	Nucleus	N_{full}	$E_{g.s.}$	Nucleus	N_{full}	$E_{g.s.}$
(n, γ)	$^{51}\mathrm{V}$	1242538	-125.54		25743302	-184.76		76528736	-236.37
(n, n)	$^{50}\mathrm{V}$	795219	-114.79		5220621	-175.73		21977271	-227.59
(n,p)	$^{50}\mathrm{Ti}$	39899	-109.86		17069465	-167.40		37534140	-218.90
(n,2n)	^{49}V	422870	-105.63		21131892	-162.56		76528736	-215.55
(n, np)	$^{49}\mathrm{Ti}$	150632	-99.24	$^{53}\mathrm{Mn}$	14123745	-158.51		90369789	-210.34
(n,2p)	$^{49}\mathrm{Sc}$	28603	-90.41	$^{53}\mathrm{Cr}$	3776746	-151.70	57 Fe	13436903	-203.30

 58 Ni $(n, \gamma)^{59}$ Ni processes. In addition to emission of γ , contributions from ejection of neutron (n) and proton (p) are also included. This leads to the possible reaction channels namely, (n, γ) , (n, n), (n, p), (n, 2n), (n, np), and (n, 2p) which require the computation of NLDs for 18 nuclei, 6 for each process. For these nuclei, we compute NLDs with pf-model space assuming 40 Ca as a core. We use GXPF1A residual interaction [42] which is well known to reproduce the binding energies, electromagnetic moments and transitions as well as excitation spectra for pf-shell nuclei.

It may be pointed out that even a smaller inaccuracy in $E_{g.s.}$ (of the order of 0.5 MeV) would cause large uncertainties in NLDs ($\sim 30\text{-}20\%$ for excitation energies \sim 5-10 MeV) that can significantly affect the reaction crosssections and astrophysical reaction rates. The accurate values of $E_{\rm g.s.}$ for the case of pf-model space are calculated using NushellX@MSU [43]. The calculation of $E_{\rm g.s.}$ turns out to be cumbersome in few cases due to large dimension corresponding to full model space (N_{full}) of the Hamiltonian matrix. In such cases, we recourse to the exponential convergence method [34]. The ground state energies obtained for several restricted model spaces are fitted to the exponential function of the form $a + be^{-cN}$. Once the parameters a, b and c are known, the exponentially converged value of $E_{\rm g.s.}$ for pf-model space can be obtained with $N=N_{full}$. For instance, in Fig. 1, the values of $E_{\rm g.s.}$ with different truncations are plotted for $^{51}\mathrm{V},~^{55}\mathrm{Fe}$ and $^{59}\mathrm{Ni}.$ We have also performed full model space calculations for $E_{g.s.}$ with full JT-space dimension $(N_{full}) \lesssim 5 \times 10^6$. The exponentially converged values for $E_{\rm g.s.}$ are found to be accurate within 0.1 MeV. In Table I, we list the values of $E_{g.s.}$ along with N_{full} for pf-model space for all the 18 nuclei relevant to the present work. Once the ground state energies are known, the NLDs are calculated within the SDM using MM code [32].

The NLDs for both the parities would require the model space consisting of single-particle states with different parities. The pf-model space can yield the NLDs only for a single parity for a given nucleus. In even-A nuclei, it will correspond to only positive parity states and those for odd-A nuclei to the negative parity states.

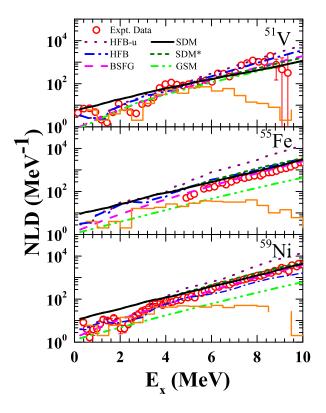


FIG. 2: Nuclear level densities as a function of excitation energies (E_x) for ^{51}V , ^{55}Fe and ^{59}Ni nuclei obtained from SDM in pf-model space by considering parity equilibration scheme (given by Eq. (6)) at $E_0{=}S_n$ and $0.8S_n$ labelled as SDM and SDM*, respectively. These results are compared with the experimental data [44–46] along with other microscopic meanfield models, HFB-u (un-normalized) and HFB as well as the phenomenological models, BSFG and GSM. Histograms represent the NLDs obtained from low-lying discrete levels [47].

Recently, Ormand and Brown [37] have estimated the values of s-wave resonance spacing D_0 for 57 Fe using the NLDs for $1/2^-$ states, instead of $1/2^+$ states, obtained within the pf-model space. The values of D_0 so deter-

TABLE II: The values of s-wave neutron resonances (D_0) are calculated for pf-model space considering parity equilibration scheme (given by Eq. (6)) at $E_0 = S_n$ and $0.8S_n$, labelled by SDM and SDM*. These results are compared with the experimental data along with other microscopic mean-field models, HFB-u (un-normalized) and HFB as well as the phenomenological models, BSFG and GSM. The neutron separation energy S_n for the product nuclei and the angular momentum $J_t^{\pi_t}$ for the target nuclei are listed.

Nucleus	$J_t^{\pi_t}$	S_n	$D_0 \; (\mathrm{keV})$							
		(MeV)	Exp.	HFB-u	$_{\mathrm{HFB}}$	BSFG	GSM	SDM	SDM^*	
$^{49}\mathrm{Ti}$	0_{+}	8.142	18.3 ± 2.9	24.6	18.6	19.1	15.2	174.4	104.9	
$^{50}\mathrm{Ti}$	$\frac{7}{2}$	10.939	4 ± 0.8	1.1	4	4.1	5.2	19.6	10.8	
$^{51}\mathrm{V}$	$\tilde{6}^{+}$	11.051	2.3 ± 0.6	0.9	1.5	2.8	4.8	6.2	3.5	
$^{53}\mathrm{Cr}$	0_{+}	7.939	43.4 ± 4.4	30.1	47.7	43	79	66.2	38.4	
$^{55}\mathrm{Fe}$	0_{+}	9.298	18 ± 2.4	5.5	15.9	16.3	104	31.7	18.4	
$^{57}\mathrm{Fe}$	0_{+}	7.646	25.4 ± 2.2	22	26.4	24.5	54.2	34.8	21.2	
$^{59}\mathrm{Ni}$	0_{+}	8.999	13.4 ± 0.9	6.1	12.8	14.1	95.7	23.8	13.9	

mined agreed reasonably with the experimental data. It was thus inferred that the parity equilibration for 57 Fe occurs near neutron separation energy (S_n) . The NLDs for $J^{\pi}=2^+$ and 2^- states extracted from the measurements of quadrupole giant resonances in 58 Ni [48] showed that parity equilibration takes place at lower energy than the predictions of SMMC calculations for $pfg_{9/2}$ model space [16, 17]. Similar conclusions were also drawn on the basis of calculations performed for sufficiently large model space [49, 50]. A simple formula [51] further suggested the parity equilibration to occur exponentially with increase in temperature. We construct the level density for positive (negative) parity for odd (even) nucleus through the parity equilibration. We use a simple scheme for the parity equilibration such as

$$\frac{\rho_{+}(E_{x})}{\rho_{-}(E_{x})} = \frac{1}{1 + e^{-\beta(E_{x} - E_{0})}}$$
(6)

where $\rho_{+}(E_{\rm x})$ and $\rho_{-}(E_{\rm x})$ are the level densities of positive and negative parities at excitation energy $E_{\rm x}$ for odd A nuclei. The ρ_{+} and ρ_{-} will be reversed for the case of even A nuclei. The parameters β and E_{0} can be adjusted to obtain required excitation energy dependence of the parity equilibration. For simplicity, we consider $\beta=1$. We obtain the NLDs using SDM with pf-model space by considering above parity equilibration scheme for $E_{0}=S_{n}$ and $0.8S_{n}$, labelled by SDM and SDM*, respectively. These NLDs are employed to calculate the D_{0} , cross-sections and reaction rates.

In Fig. 2, we show the shell model NLDs, labelled as SDM and SDM*, for ⁵¹V, ⁵⁵Fe and ⁵⁹Ni nuclei as representative examples and compare them with the existing experimental data [44–46]. The NLDs obtained from the low-lying experimental discrete levels [47] are also shown for comparison. Our calculated NLDs are in an overall agreement with the experimental data for all the three nuclei. For the comparison, we also display the NLDs obtained from Hartree-Fock-Bogoliubov (HFB) approach for Skyrme type effective force BSk14 [13]. These NLDs are obtained using combinatorial method at lower excitation energies and using statistical method at higher excitation energies. The HFB results are further normalized

to the experimental data at low energies and the neutron separation energy [13]. We also display un-normalized HFB results as labelled by HFB-u. The NLDs for HFB-u deviate noticeably for ⁵⁵Fe and ⁵⁹Ni nuclei. The curves marked by BSFG and GSM correspond to phenomenological Back-shifted Fermi gas model [11] and Generalized Superfluid model [52, 53], respectively.

The cross-sections and reaction rates, relevant to the astrophysical process are predominantly governed by the NLDs corresponding to spin and parity which determines the level spacings D_0 for s-wave neutron resonance. The D_0 can be evaluated as [13]

$$D_0 = \begin{cases} \frac{1}{\rho(S_n, J_t + 1/2, \pi_t) + \rho(S_n, J_t - 1/2, \pi_t)} & \text{for } J_t \neq 0, \\ \frac{1}{\rho(S_n, 1/2, \pi_t)} & \text{for } J_t = 0 \end{cases}$$
 (7)

where J_t and π_t are the spin and parity of target nucleus, S_n is the neutron separation energy for the product nucleus. It is evident from the Eq. (7) that the calculation of D_0 for even-even target nucleus requires the level density for $1/2^+$ in the product nucleus. Similarly, if the target is not even-even then the level densities for the product nucleus are required for the spins $J_t \pm 1/2$ and parity π_t . The values of D_0 are calculated using shell model level densities with pf-model space assuming parity equilibration scheme (Eq. (6)) for $E_0 = S_n$ and $0.8S_n$ as listed in Table II along with the available experimental data [47]. The calculations involve NLDs from 1/2⁺ states for all the nuclei presented in Table II except for 50 Ti and 51 V. The values of D_0 for 50 Ti (51 V) include the contribution from 3^- and $4^ (11/2^+$ and $13/2^+)$ spins since $J_t^{\pi} \neq 0$ for these cases. The calculated values of D_0 with $E_0 = 0.8S_n$ (SDM*) are in overall agreement with the corresponding experimental data. The exceptionally larger calculated value of D₀ for ⁴⁹Ti requires further detailed investigation. However, NLDs for this nucleus contribute to (n, np)-channel in the neutron capture by ⁵⁰V which is not a dominant one. For comparison, we display the results for D₀ obtained using some selected microscopic mean-field and phenomenological models.

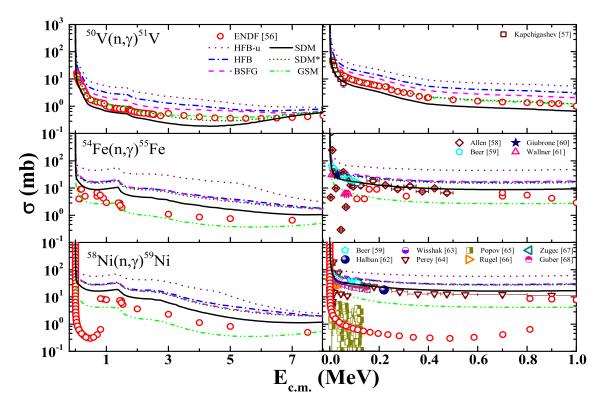


FIG. 3: Cross-sections for (n, γ) processes as a function of incident neutron energies in center-of-mass frame $(E_{\text{c.m.}})$ using NLDs from SDM and SDM* compared with those obtained from other models (as shown in Fig. 2), see text for details. Evaluated data are adopted from ENDF. The cross-sections at low $E_{\text{c.m.}}$ are shown in the right panels together with the respective experimental data.

III. (n, γ) CROSS-SECTIONS AND ASTROPHYSICAL REACTION RATES

The (n, γ) reaction cross-sections are calculated using TALYS 1.95 computer code [54] which takes into account the contributions from three major nuclear reaction mechanisms that include direct reaction, preequilibrium emission and compound nucleus. The parameters required for cross-section calculations such as the nuclear masses, discrete levels, decay schemes, OMP, and γSF are set to their default values available in TALYS. The extensive database for the NLDs obtained for various phenomenological and microscopic mean-field models are also available in TALYS. These models are the Back-shifted Fermi gas model (BSFG) [11], Gilbert and Cameron model (GC) [12], Generalized Superfluid model (GSM) [52, 53], Hartree-Fock for Skyrme type interaction with pairing treated within the Bardeen-Cooper-Schrieffer approximation (HF-BCS) [55], and Hartree-Fock-Bogoliubov for Skyrme forces (HFB) [13]. We compare the reaction cross-sections and astrophysical reaction rates obtained for some of these NLDs with the ones calculated using NLDs from SDM. The cross-sections for $^{50}{\rm V}(n,\gamma)^{51}{\rm V},\,^{54}{\rm Fe}(n,\gamma)^{55}{\rm Fe}$ and $^{58}{\rm Ni}(n,\gamma)^{59}{\rm Ni}$ reactions are calculated by including various channels as listed in Table I. Contributions from other channels which include alpha (α), deutron (d), tritium (t) and helium-3 (3 He) are found to be insignificant (not shown).

In Fig. 3, we display our theoretical estimates of

 (n,γ) cross-sections obtained from SDM NLDs corresponding to $E_0=S_n$ and $0.8S_n$ (Eq. (6)) and compare them with those obtained for NLDs from other models along with the evaluated data adopted from ENDF database (ENDF/B-VII.1) [56]. In the left panels, the results are presented for a wide range of incident neutron energy. The corresponding zoomed versions for the lower energies up to 1 MeV, relevant to astrophysical reaction rates at temperatures up to the order of GK, are presented in the right panels. The cross-sections based on the NLDs from SDM are in an overall agreement with the evaluated data (left panels) as well as available experimental data from various groups (right panels) [57–68]. For the low incident neutron energies, our SDM results are in agreement with the experimental data which emphasizes the role of residual interaction in the astrophysical regime. Also, the results from HFB, BSFG and GSM are found to be in a reasonable agreement with the experimental cross-sections as the NLDs for these models are appropriately normalized with the measured ones. However, the results obtained by HFB-u, which correspond to unnormalized NLDs, show noticeable deviations from the measured cross-sections for neutron capture reactions.

For the reaction network, one needs astrophysical reaction rates as one of the inputs. Once the variation of cross-section with energy is known, the astrophysical reaction rates $N_A < \sigma v >$ can be computed with N_A being the Avogadro number and $< \sigma v >$ is the Maxwellian average, where v is the relative velocity of neutron.

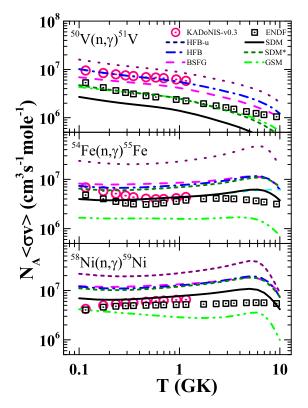


FIG. 4: The astrophysical reaction rates as a function of temperature using NLDs from SDM and SDM* compared with those obtained for other models (as shown in Fig. 2). For comparison, the recommended values from ENDF [56] and 'KADoNiS v0.3' [69] are shown. For the case of 50 V $(n, \gamma)^{51}$ V, KADoNiS estimates are purely theoretical.

These averages are computed at a fix temperature which ranges from 0.1 GK to 10 GK. For these temperatures, cross-sections at energies within the range of few keV to \sim 1 MeV contribute maximally. We show in Fig. 4, the astrophysical reaction rates obtained by using the NLDs from SDM and compare them with the recommended values from ENDF [56] and 'KADoNiS v0.3' [69]. These results are basically the Maxwellian average of cross-sections shown in Fig. 3. The results from HFB, BSFG and GSM are also shown for comparison. SDM results with $0.8S_n \leq E_0 \leq S_n$ explain quite well the recommended values from ENDF [56] in all the cases.

IV. SUMMARY AND OUTLOOK

We obtain realistic NLDs within the framework of spectral distribution method applied to many-body shell

model Hamiltonian for pf-model space. A particular attention has been paid to calculate the accurate ground state energy since it is a crucial input in the SDM calculations. To incorporate the NLDs of opposite parities in pf-model space, an appropriate parity equilibration scheme has been used. The NLDs so obtained and s-wave neutron resonance spacings agree reasonably well with the available experimental data. We further compute reaction cross-sections and astrophysical reaction rates for the neutron capture processes such as $^{50}V(n,\gamma)^{51}V$, 54 Fe $(n,\gamma)^{55}$ Fe and 58 Ni $(n,\gamma)^{59}$ Ni. The calculated reaction cross-sections are found to be in harmony with experimental data, particularly for the incident neutron energies of astrophysical interest. Similar is the case for the astrophysical reaction rates, for the temperature ranging from 0.1 - 10 GK.

Since the present method is quite general and naturally accounts for the collective excitations, therefore, it can be explored in various model spaces and other reactions of astrophysical interest. To obtain the realistic shell-model NLDs of both parities naturally, it would be desirable to perform calculations with larger model spaces which involve huge computation. It would be worthwhile to study the astrophysical reaction rates using shell model NLDs for the neutron-rich nuclei away from the line of β -stability where the level density may deviate significantly compared to the nearby stable nuclei [9, 70, 71]. Experiments along this direction using inverse kinematics at radioactive ion beam facilities are expected to be operational in near future.

Acknowledgments

We are thankful to P. C. Srivastava and R. Senkov for some inputs of the shell model calculations. We also express our gratitude to Pratap Roy for fruitful discussions. TG acknowledges Council of Scientific and Industrial Research (CSIR), Government of India for fellowship Grant No. 09/489(0113)/2019-EMR-I. BM acknowledges the financial support from the Croatian Science Foundation and the École Polytechnique Fédérale de Lausanne, under the project TTP-2018-07-3554 "Exotic Nuclear Structure and Dynamics", with funds of the Croatian-Swiss Research Programme. She also acknowledges the support received from IIT Ropar, India where a part of this work has been carried out. BKA acknowledges partial support from the Department of Science and Technology, Government of India with grant no. CRG/2021/000101.

^[1] J. J. P. de Lima, Eur. J. Phys. 19, 485 (1998).

^[2] M. Prelas, M. Boraas, F. D. L. Torre Aguilar, J. D. Seelig,

M. T. Tchouaso, and D. Wisniewski, Springer Cham **56**, 1518 (2016).

- [3] E. M. Burbidge, G. R. Burbidge, W. A. Fowler, and F. Hoyle, Rev. Mod. Phys. 29, 547 (1957).
- [4] B. P. Abbott, R. Abbott, T. D. Abbott, F. Acernese, K. Ackley, C. Adams, T. Adams, P. Aesso, R. X. Adhikari, V. B. Adya, et al. (LIGO Scientific Collaboration and Virgo Collaboration), Phys. Rev. Lett. 119, 161101 (2017).
- [5] I. Arcavi et al., Nature 551, 64 (2017).
- [6] E. Pian et al., Nature **551**, 67 (2017).
- [7] P. Hill and Y. Wu, Phys. Rev. C 103, 014602 (2021).
- [8] W. Hauser and H. Feshbach, Phys. Rev. 87, 366 (1952).
- [9] S. N. Liddick, A. Spyrou, B. P. Crider, F. Naqvi, A. C. Larsen, M. Guttormsen, M. Mumpower, R. Surman, G. Perdikakis, D. L. Bleuel, et al., Phys. Rev. Lett. 116, 242502 (2016).
- [10] S. Dutta, G. Gangopadhyay, and A. Bhattacharyya, Phys. Rev. C 94, 054611 (2016).
- [11] W. Dilg, W. Schantl, H. Vonach, and M. Uhl, Nucl. Phys. A 217, 269 (1973).
- [12] A. Gilbert and A. G. W. Cameron, Can. Jour. of Phys. 43, 1446 (1965).
- [13] S. Goriely, S. Hilaire, and A. J. Koning, Phys. Rev. C 78, 064307 (2008).
- [14] C. W. Johnson, S. E. Koonin, G. H. Lang, and W. E. Ormand, Phys. Rev. Lett. 69, 3157 (1992).
- [15] G. H. Lang, C. W. Johnson, S. E. Koonin, and W. E. Ormand, Phys. Rev. C 48, 1518 (1993).
- [16] H. Nakada and Y. Alhassid, Phys. Rev. Lett. 79, 2939 (1997).
- [17] H. Nakada and Y. Alhassid, Phys. Lett. B 436, 231 (1998).
- [18] H. Nakada and Y. Alhassid, Phys. Rev. C 78, 051304(R) (2008).
- [19] Y. Alhassid, M. Bonett-Matiz, S. Liu, and H. Nakada, Phys. Rev. C 92, 024307 (2015).
- [20] F. Chang, J. French, and T. Thio, Ann. Phys. 66, 137 (1971).
- [21] J. B. French and K. F. Ratcliff, Phys. Rev. C 3, 94 (1971).
- [22] V. K. B. Kota and K. Kar, Pramana J. Phys. 32, 647 (1989).
- [23] V. Kota and D. Majumdar, Nucl. Phys. A 604, 129 (1996).
- [24] M. Horoi, J. Kaiser, and V. Zelevinsky, Phys. Rev. C 67, 054309 (2003).
- [25] M. Horoi, M. Ghita, and V. Zelevinsky, Phys. Rev. C 69, 041307(R) (2004).
- [26] K. Kar, A. Ray, and S. Sarkar, Astrophys. J. 434, 662 (1994).
- [27] V. K. B. Kota and D. Majumdar, Z. Phys. A Hadrons nucl. 351, 377 (1995).
- [28] J. Gómez, K. Kar, V. Kota, R. Molina, A. Relaño, and J. Retamosa, Phys. Rep. 499, 103 (2011).
- [29] V. K. B. Kota and N. D. Chavda, Int. J. Mod. Phys. E 27, 1830001 (2018).
- [30] R. A. Sen'kov and M. Horoi, Phys. Rev. C 82, 024304 (2010).
- [31] M. Horoi and R. Senkov, PoS NIC XI, 222 (2011).
- [32] R. Sen'kov, M. Horoi, and V. Zelevinsky, Comp. Phys. Comm. 184, 215 (2013).
- [33] R. Sen'kov and V. Zelevinsky, Phys. Rev. C 93, 064304 (2016).
- [34] M. Horoi, B. A. Brown, and V. Zelevinsky, Phys. Rev. C 65, 027303 (2002).
- [35] Z.-C. Gao and M. Horoi, Phys. Rev. C **79**, 014311 (2009).

- [36] Z.-C. Gao, M. Horoi, and Y. S. Chen, Phys. Rev. C 80, 034325 (2009).
- [37] W. E. Ormand and B. A. Brown, Phys. Rev. C 102, 014315 (2020).
- [38] K. Mon and J. French, Ann. Phys. 95, 90 (1975).
- [39] T. A. Brody, J. Flores, J. B. French, P. A. Mello, A. Pandey, and S. S. M. Wong, Rev. Mod. Phys. 53, 385 (1981).
- [40] S. Wong, Nuclear Statistical Spectroscopy (Oxford University Press USA, 1986).
- [41] V. K. B. Kota, R. u. Haq, and D. Koltun, Spectral Distributions in Nuclei and Statistical Spectroscopy (WORLD SCIENTIFIC, 2010).
- [42] M. Honma, T. Otsuka, B. A. Brown, and T. Mizusaki, Phys. Rev. C 69, 034335 (2004).
- [43] B. Brown and W. Rae, Nucl. Data Sheets 120, 115 (2014).
- [44] A. C. Larsen, R. Chankova, M. Guttormsen, F. Ingebretsen, S. Messelt, J. Rekstad, S. Siem, N. U. H. Syed, S. W. Ødegård, T. Lönnroth, et al., Phys. Rev. C 73, 064301 (2006).
- [45] A. P. D. Ramirez, A. V. Voinov, S. M. Grimes, Y. Byun, C. R. Brune, T. N. Massey, S. Akhtar, S. Dhakal, and C. E. Parker, Phys. Rev. C 92, 014303 (2015).
- [46] A. V. Voinov, S. M. Grimes, C. R. Brune, T. Massey, and A. Schiller, EPJ Web Conf. 21, 05001 (2012).
- [47] R. Capote, M. Herman, P. Obložinský, P. Young, S. Goriely, T. Belgya, A. Ignatyuk, A. Koning, S. Hilaire, V. Plujko, et al., Nucl. Data Sheets 110, 3107 (2009).
- [48] Y. Kalmykov, C. Özen, K. Langanke, G. Martínez-Pinedo, P. von Neumann-Cosel, and A. Richter, Phys. Rev. Lett. 99, 202502 (2007).
- [49] D. Mocelj, T. Rauscher, G. Martínez-Pinedo, K. Langanke, L. Pacearescu, A. Faessler, F.-K. Thielemann, and Y. Alhassid, Phys. Rev. C 75, 045805 (2007).
- [50] K. V. Houcke, S. M. A. Rombouts, K. Heyde, and Y. Alhassid, Phys. Rev. C 79, 024302 (2009).
- [51] Y. Alhassid, G. F. Bertsch, S. Liu, and H. Nakada, Phys. Rev. Lett. 84, 4313 (2000).
- [52] A. V. Ignatyuk, K. K. Istekov, and G. N. Smirenkin, Sov. J. Nucl. Phys. 29, 450 (1979).
- [53] A. V. Ignatyuk, J. L. Weil, S. Raman, and S. Kahane, Phys. Rev. C 47, 1504 (1993).
- [54] A. Koning, S. Hilaire, and S. Goriely, TALYS-1.95 (2020), http://www.talys.eu/download-talys/.
- [55] P. Demetriou and S. Goriely, Nucl. Phys. A 695, 95 (2001).
- [56] Evaluated Nuclear Data Files (ENDF/B-VII.1), https://www-nds.iaea.org/exfor/endf.htm; https://www.nndc.bnl.gov/astro/.
- [57] S. Kapchigashev, Atomnaya Energiya 19, 294 (1965).
- [58] B. Allen, A. de L. Musgrove, J. Boldeman, and R. Macklin, Nucl. Phys. A 283, 37 (1977).
- [59] H. Beer and R. Spencer, Nucl. Phys. A 240, 29 (1975).
- [60] G. Giubrone, C. Domingo-Pardo, J. Taín, C. Lederer, S. Altstadt, J. Andrzejewski, L. Audouin, M. Barbagallo, V. Bécares, F. Bečvař, et al., Nucl. Data Sheets 119, 117 (2014).
- [61] A. Wallner, K. Buczak, T. Belgya, M. Bichler, L. Co-quard, I. Dillmann, R. Golser, F. Käppeler, A. Karakas, W. Kutschera, et al., Phys. Rev. C 96, 025808 (2017).
- [62] H. V. Halban and L. Kowarski, Nature 142, 392 (1938).
- [63] K. Wisshak, F. Käppeler, G. Reffo, and F. Fabbri, Nucl.

- Sci. Eng. 86, 168 (1984).
- [64] C. M. Perey, F. G. Perey, J. A. Harvey, N. W. Hill, N. M. Larson, R. L. Macklin, and D. C. Larson, Phys. Rev. C 47, 1143 (1993).
- [65] Y. P. Popov, A. V. Voinov, S. S. Parzitski, N. A. Gundorin, D. G. Serov, A. P. Kobzev, and P. V. Sedyshev, Phys. At. Nucl. 63, 525 (2000).
- [66] G. Rugel, I. Dillmann, T. Faestermann, M. Heil, F. Käppeler, K. Knie, G. Korschinek, W. Kutschera, M. Poutivtsev, and A. Wallner, Nucl. Instrum. Methods Phys. Res. B 259, 683 (2007).
- [67] P. Žugec, M. Barbagallo, N. Colonna, D. Bosnar, S. Altstadt, J. Andrzejewski, L. Audouin, V. Bécares, F. Bečvář, F. Belloni, et al. (The n_TOF Collaboration),

- Phys. Rev. C 89, 014605 (2014).
- [68] K. H. Guber, H. Derrien, L. C. Leal, G. Arbanas, D. Wiarda, P. E. Koehler, and J. A. Harvey, Phys. Rev. C 82, 057601 (2010).
- [69] I. Dillmann, M. Heil, F. Käppeler, R. Plag, T. Rauscher, and F. Thielemann, AIP Conf. Proc. 819, 123 (2006), https://kadonis.org/.
- [70] S. I. Al-Quraishi, S. M. Grimes, T. N. Massey, and D. A. Resler, Phys. Rev. C 63, 065803 (2001).
- [71] P. Roy, K. Banerjee, T. K. Rana, S. Kundu, S. Manna, A. Sen, D. Mondal, J. Sadhukhan, M. T. Senthil Kannan, T. K. Ghosh, et al., Phys. Rev. C 102, 061601(R) (2020).